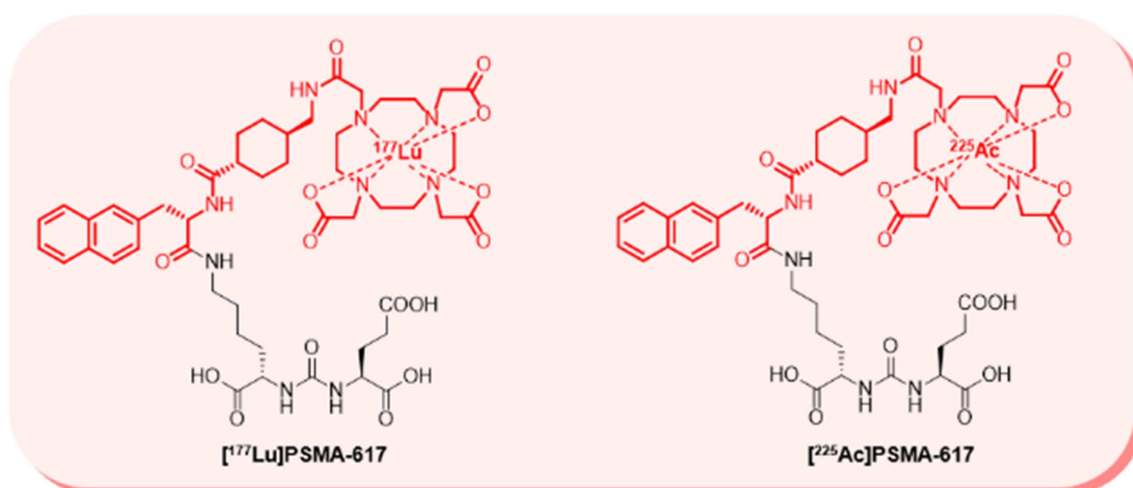
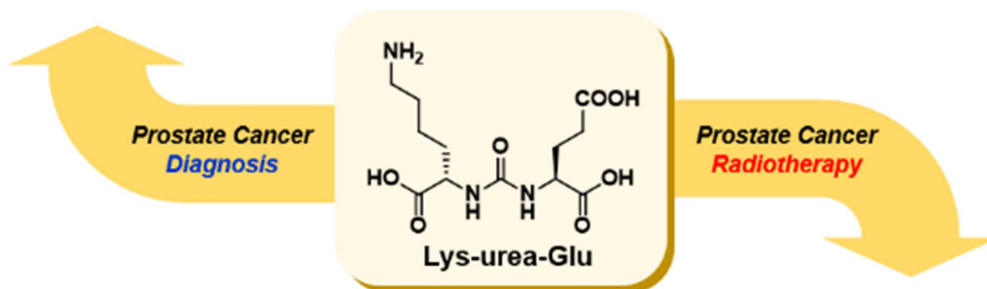
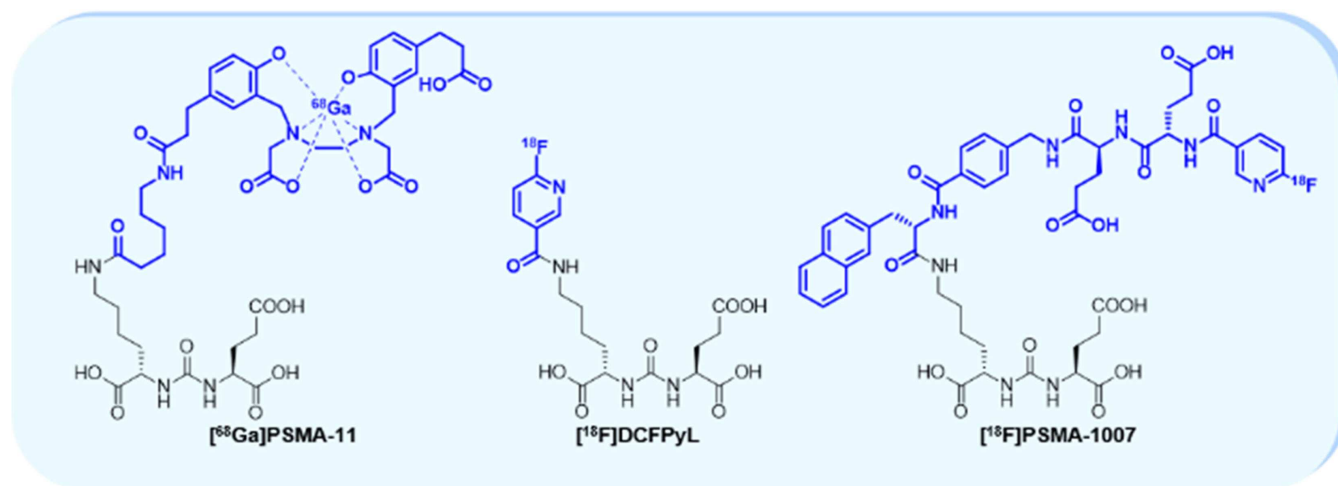


Special
Issue

Prostate-Specific Membrane Antigen (PSMA)-Targeted Radionuclide Probes for Imaging and Therapy of Prostate Cancer

Hongmok Kwon, Sang-Hyun Son, and Youngjoo Byun*^[a]



Abstract: Prostate cancer (PCa) is one of the common cancers among men. Despite the prevalence of PCa, there are still unmet medical needs in the diagnosis and treatment of metastatic prostate cancer. Prostate-specific membrane antigen (PSMA) is a type II zinc-dependent metalloprotease which is highly overexpressed in metastatic PCa. In the last several years, PCa imaging probes targeting PSMA have been

developed in academia as well as in industry. Among them, low molecular weight PSMA-targeted ligands based on the Glu-urea-Lys scaffold have been evaluated in preclinical and clinical studies. This review provides an overview of the recent development in PSMA-targeted imaging or therapeutic probes for metastatic PCa.

1. Introduction

Prostate cancer (PCa) is one of the most prevalently diagnosed cancers in Europe and USA. It is the second leading cause of cancer-related death in men.^[1] Localized primary PCa can be treated effectively with current treatment options including surgery, chemotherapy, and radiation. However, when PCa metastasizes to the lymph nodes or bones, the mortality rate increases dramatically.^[2] Current diagnosis of PCa is generally performed by examining blood prostate-specific antigen (PSA) level, followed by digital rectal exam by clinical experts. However, clinical studies showed that even 10–20% of PCa cases were diagnosed as such even when the PSA level is lower than the control baseline.^[3] Non-invasive and sensitive molecular imaging techniques, PET and SPECT, have gained favor over PSA detection with regards to their predictive capacity in detecting the small lesions of metastatic PCa. In particular, the recurrence site of PCa patients with low PSA levels can be localized by using PSMA radionuclide imaging.

Prostate-specific membrane antigen (PSMA) is a type II zinc-dependent protease that is overexpressed on the surface of androgen-independent PCa cells.^[4] The expression level of PSMA correlates with the stage and grade of the tumor.^[4b,5] PSMA has an extracellular ligand-binding domain, transmembrane region, and a short cytosol region. Binding of the ligand to PSMA leads to the internalization of the complex, mediated by clathrin-dependent endocytosis mechanism.^[6] The aforementioned features of PSMA, such as the presence of ligand-binding motif in the extracellular region and ligand internalization, indicate that it is an excellent target protein for PCa diagnosis or treatment.

The ¹¹¹In-labeled monoclonal antibody, ProstaScint®, is the only PSMA-targeted radiopharmaceutical agent for PCa diagnosis approved by FDA. However, there are some limitations associated with this antibody, such as prolonged blood circulation time and restricted access to epitope in PSMA.^[7] On the contrary, low molecular weight (MW) compounds labeled with radionuclides have the ability to detect PSMA more precisely. Among the PSMA-targeted small molecules, the Lys-urea-Glu analogs, which were first synthesized by Kozikowski

group in 2001^[8], have been extensively exploited as imaging and therapy probes due to synthetic feasibility and maintenance of high PSMA-binding affinity.^[9]

In this review, we provide an overview of the recent progress on PSMA-targeted radionuclide probes in the last several years.

2. PSMA-Targeted Small Molecules Advanced to Clinical Applications

2.1. [¹⁸F]DCFPyL

Pomper and his co-workers reported that radiolabeled Cys-urea-Glu analogs, [¹¹C]DCMC and [¹⁸F]DCFBC, showed good tumor-to-background ratio and had a potential as PSMA-targeted imaging probes.^[10] However, due to the instability of the thiol group in the precursors of [¹¹C]DCMC and [¹⁸F]DCFBC, they designed and synthesized more stable Lys-urea-Glu analogs, 2-(3-{1-carboxy-5-[(6-¹⁸F]fluoropyridine-3-carbonyl)-amino]-pentyl}-ureido)-pentanedioic acid ([¹⁸F]DCFPyL, **1** in Figure 1).^[11] Lys residue of the PSMA-binding motif was reacted with [¹⁸F]F-Py-TFP (6-¹⁸F]fluoronicotinic acid 2,3,5,6-tetra-fluorophenyl ester) to provide [¹⁸F]DCFPyL with radiochemical yields of 36–53% (decay corrected).^[11] As it exhibited strong PSMA binding affinity for PSMA ($K_i = 1.1 \pm 0.1$ nM) and high uptake in PSMA-positive PC3 PIP tumors ($39.4 \pm 5.4\%$ ID/g), compound **1** rapidly progressed to clinical trials. Compound **1** detected a prominent intraprostatic focus of PCa in a prospective cohort of six men.^[12] In 2018, Allaf and his colleagues performed phase II single-center study using **1**.^[13] Patients with localized disease and at high risk of harboring metastatic PCa in the pre-operative stage were imaged by positron emission tomography-computed tomography (PET/CT). The surgical pathology was used as a diagnostic standard for PET/CT image analysis. The two blinded nuclear medicine readers involved in the imaging study of compound **1** exhibited a high degree of concordance with respect to the detection of the sites of disease. The uptake sites of compound **1** were successfully identified in all imaged patients.

2.2. [⁶⁸Ga]PSMA-11

Due to favorable radionuclide characteristics (positron-emitting fraction = 89%, $t_{1/2} = 68$ min, mean value of maximum positron

[a] H. Kwon, Dr. S.-H. Son, Prof. Y. Byun
College of Pharmacy
Korea University
2511 Sejong-ro, Sejong 30019 (South Korea)
E-mail: yjbyun1@korea.ac.kr



This manuscript is part of a special issue dedicated to researchers in Korea. Click here to see the Table of Contents of the special issue.

energy = 0.89 MeV), ^{68}Ga has emerged as important radionuclide for PET imaging of tumor.^[14] Facile radionuclide production of ^{68}Ga from in-house $^{68}\text{Ge}/^{68}\text{Ga}$ generator led to the increased use of ^{68}Ga instead of cyclotron-based isotopes such as ^{18}F or ^{124}I .^[15] The Lys-urea-Glu motif was conjugated with ^{68}Ga -labeled lipophilic HBED-CC (*N,N'*-bis[2-hydroxy-5-(carboxyethyl)-benzyl]ethylenediamine *N,N'*-diacetic acid) chelator to generate [^{68}Ga]PSMA-11 (**2** in Figure 1).^[16] Compound **2** exhibited excellent PSMA binding affinity (IC_{50} in enzyme-based assay: 7.5 ± 2.2 nM; K_i determined in cell-based assay: 12.0 ± 2.8 nM). Compound **2** exhibited greater performance in detecting typical PCa lesions in patients with low PSA level than ^{18}F -fluoromethylcholine.^[17] Clinical studies with 319 patients demonstrated a patient-level sensitivity of 82.8% which correlated with the histopathology.^[18] The detection rate of compound **2** was associated with the clinical stage of BCR (biochemical recurrence).^[19] After radical prostatectomy, the detection rate was 64.5% in the subgroup of patients with persisting detectable PSA after radical prostatectomy. In addition, the sensitivity of **2** was also higher than that of standard imaging.^[20] In the subgroup, 74% of the patients with no lesions on abdominopelvic CT and bone scan (199 patients) exhibited PSMA-positive lesions by **2** PET/CT imaging. In addition, 16 patients (41%) in the subgroup with oligometastatic lesions on abdominopelvic CT and bone scan (39 patients) were confirmed as upstaged polymetastatic disease. The positive correlation between the positivity and PSA levels of compound **2** was also verified in this study. The prospective clinical trial of preoperative PCa lymph node (LN) staging using compound **2** was carried out and analyzed in combination with the histopathology data.^[21] PET/CT using **2** showed moderate sensitivity (56%) despite the high specificity (98%) in the LN-region-based analysis. A randomized prospective phase III trial to evaluate the success rate of salvage radiotherapy planned by PET/CT with **2** is now underway.

2.3. PSMA-617

Although compound **2** rapidly progressed to clinical studies, there are several demands to improve ^{68}Ga -chelating PSMA ligand **2**. In particular, chelator HBED-CC has a limitation for general use because it forms unstable complexes with therapeutic radionuclides including ^{177}Lu , ^{90}Y , and ^{225}Ac . As an alternative, PSMA-617 (**3**, Figure 1) consists of PSMA-binding Glu-urea-Lys motif, DOTA chelator, and linker with tranexamic acid and 2-naphthylalanine.^[22] The radiochemical yields of compounds **3a-3b** were pretty high (97% for **3a**, 99% for **3b**). According to the *in vitro* LNCaP cell-based assay, unlabeled **3** displayed strong binding affinity for PSMA in nanomolar range ($K_i = 2.34 \pm 2.94$ nM). The radiolabeled compounds **3a** and **3b** also showed comparable binding affinities for PSMA (6.40 ± 1.02 nM for **3a**, 6.9 ± 1.32 nM for **3b**). Compound **3a** showed high tumor-to-background ratios (tumor/blood = 1,058, tumor/muscle = 529). Compound **3** emerged as a promising radio-tracer for PCa diagnostic application. Both β - and α -particle

emitting radionuclides could be introduced into compound **3** for the purpose of PCa therapy.

A retrospective study evaluated the efficacy and safety of β -emitting **3b** for patients with metastatic castration-resistant prostate cancer (mCRPC).^[23] All patients were treated with **3b** every 8 weeks until progression, death or withdrawal, and 33% of patients showed a PSA decline $\geq 50\%$ after the first cycle. A single-center, single-arm, phase II clinical study showed an improvement in the general health status of **3b**-treated patients.^[24]

Emitted α -particle in the body transfers high linear energy to cells with short path length, which leads to a higher likelihood of DNA strands breakdown.^[25] PSMA mediates tumor cell internalization upon binding with ligands, and hence, it is a promising target for α -particle radiotherapy.^[4b,6a,26] Actinium-225 emits four α -particles and has considerably long half-life (10 days), and hence, it is regarded as a promising therapeutic radionuclide.^[27]

^{225}Ac -labeled PSMA-617 (**3c**) was evaluated as α -particle radiotherapy tool. In the clinical trial of first-in-human treatment with two mCRPC patients,^[28] **3c** exhibited significant benefit to

Hongmok Kwon was born and raised in Seoul, South Korea. He graduated from the Korea University College of Pharmacy with his Pharm.D. degree. He is currently pursuing his Ph.D. at the same school under the guidance of Prof. Y. Byun. His research interests include design and synthesis of small-molecule ligands for binding prostate cancer biomarkers such as hepsin or PSMA.



Sang-Hyun Son received his PhD degree from Hokkaido University in 2008 under the supervision of prof. N. Sakairi and did his postdoctoral training at RIKEN with prof. Y. Ito (Japan). In 2015, he joined prof. Y. Byun group at Korea University College of Pharmacy as a postdoctoral fellow. His research focused on the development of small molecule ligands against a variety of targets.



Youngjoo Byun received his Ph.D degree from Ohio State University, Ohio. After post-doctoral training under the supervision of Dr. Martin G Pomper at Johns Hopkins University, he joined College of Pharmacy, Korea University in 2011. Currently, he is the director of Institute of Pharmaceutical Sciences and Translational Research (IPSTR), and a full professor at Korea University.



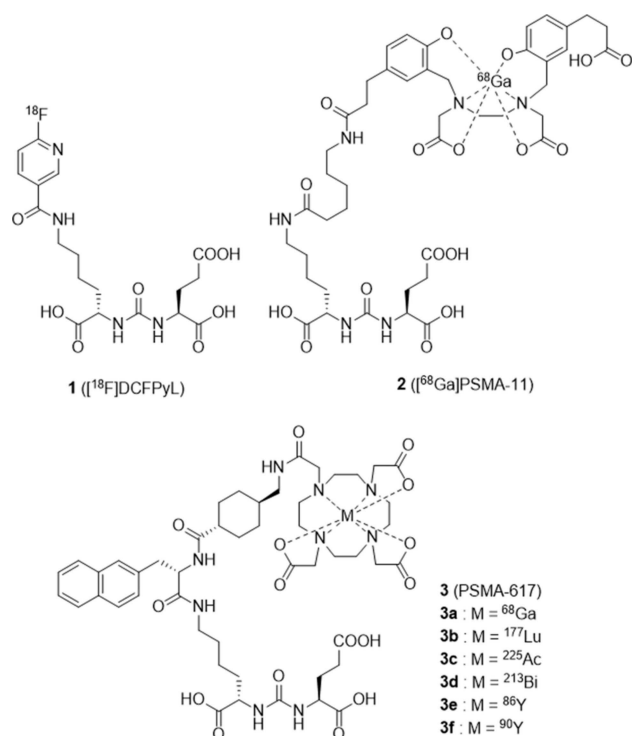


Figure 1. PSMA ligands in clinical trials

both patients. Both patients showed significant decline of PSA level and complete therapy response as observed from the images of PET/CT scanning. In another study with advanced metastatic PCa patients, $\geq 90\%$ PSA decline was observed in 14 of 17 patients after treatment with 3c.^[29] In a clinical trial with ^{213}Bi -chelated ligand (3d) for metastatic PCa patients, only a case of partial remission was observed^[30] with 3d exhibiting an inferior therapeutic index compared to 3c.^[31]

3. ^{18}F -Labeled Radiotracers

Despite that ^{68}Ga -chelated PSMA-binding agents have been actively developed, ^{18}F is still the most common radionuclide for PET scanning because it has advantages over ^{68}Ga with respect to the longer half-life (109.8 min for ^{18}F vs 67.7 min for ^{68}Ga), greater efficiency of positron emission (97% for ^{18}F vs 89% for ^{68}Ga), availability of large-scale cyclotron production, and minimal modification of ligand structure via bioisosterism with hydrogen atom.^[32]

Although ^{18}F]DCFPyL has advanced clinical translation, its substantial uptake by non-target organs such as kidney and salivary gland may result in dose-limiting toxicities.^[33] Furthermore, the radiochemical synthesis process needs to be improved due to its low radiochemical yield.^[33] In addition, the problem of fast washout from tumor also needs to be overcome.^[11] As an attempt to improve tumor-to-background ratio, Neumaier group made structural modifications of 1 by introducing the methoxy group in the pyridine ring (4 in Figure 2).^[34] *In vitro* uptake of 4 in LNCaP cells was significantly

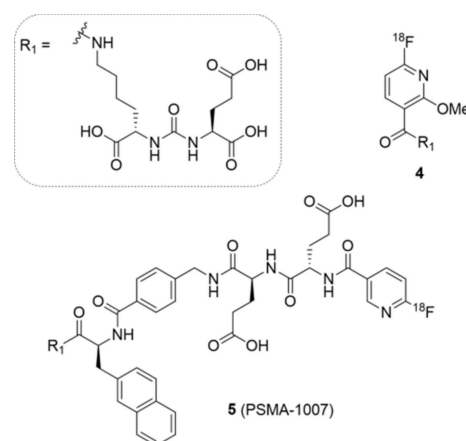


Figure 2. Radiotracers labeled with ^{18}F to pyridine ring

higher than that of 1. In an *in vivo* study with rats expressing PSMA-positive superior cervical ganglia, there was an improved tumor-to-background ratio of 4 (8.15 ± 1.71) compared to 1 (6.38 ± 1.87). However, the liver uptake of 4 was higher than that of 1, due to the increased lipophilicity by the methoxy group.

Kopka group developed ^{18}F]PSMA-1007 (5 in Figure 2) by using ^{18}F]F-Py-TFP as a prosthetic group for PET imaging.^[35] They established automatic radio-synthesis procedure which passed quality control standards. Compound 5 turned out to be a potent and promising PET-imaging probe of PSMA. It maintained the key linker structure of compound 3 in order to maintain the biodistribution behavior of 3. The 2-naphthyl-L-alanine as a linker for compounds 3 and 5 provided a rigid conformation and aromatic ring to enhance the PSMA-binding affinity *in vitro* and tumor uptake *in vivo*.^[22] The tumor uptake of 5 in the LNCaP cell line was $8.0 \pm 2.4\%$ ID/g at 1 h p.i. (post-injection), and the uptake in the non-target tissues except for spleen and kidney was low. In the biodistribution study^[36], compound 5 showed slower tumor accumulation than compound 3, but less crucial because of relatively longer half-life of ^{18}F than ^{68}Ga . Tumor tissue uptake was improved, contributing to the easy detection of small lymph node metastases (94.7% sensitivity, 100% specificity). Interestingly, unlike compounds 1–3, which are rapidly excreted in the urinary tract, compound 5 showed hepatobiliary clearance. Such characteristic of 5 facilitated the detection of local PCa recurrence.^[36] In addition, slow blood clearance of 5 was observed due to electrostatic interactions of 5 with serum albumin.^[34,37] As high blood protein binding delays the excretion of the tracer and inhibits the accumulation of the kidneys and bladder, 5 could have an advantage in the detection of PCa metastases adjacent to urethra and bladder. To investigate detection efficacy of 5 with other tracers, the retrospective analysis of clinical trials involving 251 patients with BCR after radical prostatectomy (RP) were conducted.^[38] In this study, 81.3% of patients exhibited evidence of recurrence on PET/CT. The detection rates of 5 PET/CT were 94.0% (PSA level ≥ 2 ng/mL), 90.9% (2 ng/mL > PSA

level ≥ 1 ng/mL), 74.5% (1 ng/mL > PSA level ≥ 0.5 ng/mL), respectively.

Besides ^{18}F -labeled pyridine ring, there have been reports of ^{18}F -labeled PSMA ligands synthesized by click chemistry. Pomper group synthesized the PSMA inhibitor substituted with [^{18}F]fluoroethyl triazole (**6**^[39], Figure 3) using 1,3-dipolar cycloaddition reaction.^[40] Compound **6** was prepared in mild conditions with high yield (total synthetic time: 60 min, decay-uncorrected radiochemical yield: 14%). However, *in vivo* distribution studies revealed that PSMA-positive PC3 PIP tumor uptake of **6** ($40.31 \pm 5.13\%$ ID/g at 30 min, $25.74 \pm 7.33\%$ ID/g at 4 h) was lower than that of **1** ($84.29 \pm 12.29\%$ ID/g at 1 h). It may be due to low binding affinity of **6** for PSMA (K_i of **6**: 12.9 nM, **1**: 1.1 nM). In addition, the hydrophobic interactions of the fluoro-aryl group of **1** in S1 sub-pocket were greater than that of the fluoroethyl triazole of **6**.^[41] However, due to overall lower uptake in normal organs and faster clearance than **1**, compound **6** exhibited higher tumor-to-kidney ratio (4:1 for **6** and 1:1 for **1** at 2 h p.i.).

Fluoroethyltriazolylphenyl urea-based PSMA ligands were reported by Babich and his co-workers.^[32] They conjugated 2- [^{18}F]fluoroethylazide with an alkyne precursor by applying Cu(I)-catalyzed click chemistry. The phenylurea moiety of the prosthetic group was retained because it displayed improved potency at PSMA inhibitor MIP-1095 (**7**) relative to its amide analogue.^[42] 1,2,3-triazole ring was used as bioisostere of amide

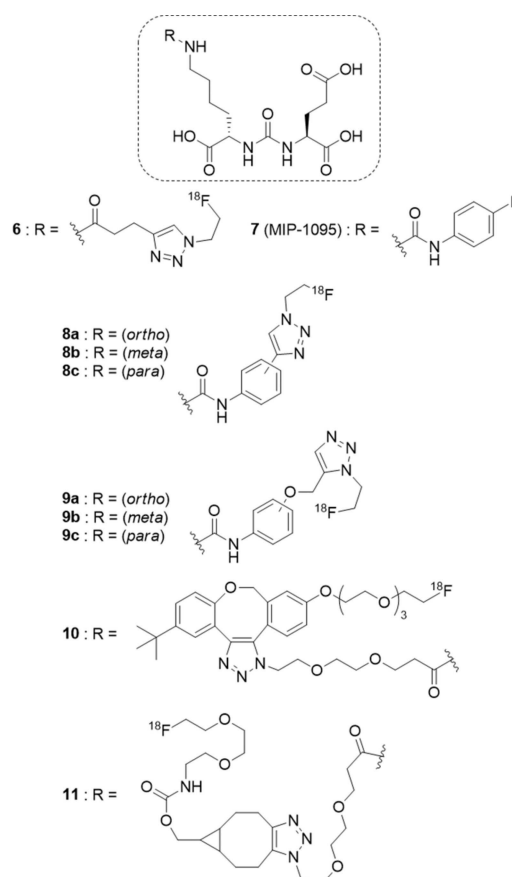


Figure 3. ^{18}F -labeled radiotracers conjugated with click chemistry

group^[43] and fluoroethyl moiety resided more deeply into the S1 hydrophobic subpocket. Compounds **8a–8c** showed higher binding affinities for PSMA and tumor uptake than triazolymethoxy analogs **9a–9c**, indicating that S1 subpocket is sensitive to the bulkiness and flexibility of the moiety. Optimal volume and rotational rigidity of linker in compounds **8a–8c** might contribute to increase of PSMA binding affinity and tumor uptake.^[44] Compound **8b** showed the highest image contrast and tumor-to-background ratio among the triazolyl analogs. The tumor-to-blood ratio for **8b** was 28.8 ± 8.06 at 1 h post-injection.

Although Cu(I)-catalyzed azide-alkyne cycloaddition has become an attractive conjugation method in the synthesis of radiotracers^[45], it sometimes causes oligonucleotide and polysaccharide degradation *in vivo* due to the nature of Cu(I) and complicated quality control measures for the final compound.^[46] Li and his colleagues adapted strain-promoted copper-free azide-alkyne cycloaddition for the preparation of ^{18}F -PET probe. They successfully conjugated ^{18}F -labeled cycloalkyne compounds with azide-functionalized Lys-urea-Glu.^[47] The reaction rate was much faster in compound **10** (rt, 5 min) than in compound **11** (80 °C, 15 min). The IC_{50} values of **10** and **11** were 108.9 nM and 156.4 nM, respectively, similar to that of **3** (144.6 nM). Compound **11** exhibited better tumor uptake ($2.24 \pm 0.03\%$ ID/g at 2 h p.i.) and higher tumor-to-background ratio (tumor-to-liver: 5.83 ± 1.5 , tumor-to-muscle: 69.59 ± 7.23) than compound **10**.

It was reported that the fluorinase enzyme isolated from *Streptomyces cattleya* selectively incorporated fluoride ion at the C-5 position of 5'-chloro-5'-deoxyadenosine (5'-CIDA).^[48] Using this methodology, O'Hagan and co-workers achieved ^{18}F -radio-labeling of PSMA agent by applying fluorinase-mediated transhalogenation reaction in aqueous buffered media (pH 7.8).^[49] The radiochemical yield of **12** was 3.4% (decay uncorrected), which was similar to those of other previously reported fluorinase catalyzed radiolabeling.^[50] IC_{50} value of **12** from an *in vitro* fluorescence-based assay was 98.6 ± 22.5 nM.

Yang and co-workers introduced 1,4,7-triazaclononane-1,4,7-triacetic acid (NOTA) instead of 1,4,7,10-tetraazacyclododecane-1,4,7,10-tetraacetic acid (DOTA) in the chelator position of compound **3** and used Al^{18}F as an ^{18}F -labeling reagent.^[51] Al^{18}F chelation allows ^{18}F -labeling to be performed in milder conditions and in shorter time.^[52] Compound **13** (Figure 4) was prepared with high non-decayed radiochemical yield ($32.2 \pm 4.5\%$) within 30 min. Dissociation of $^{18}\text{F}^-$ ion from compound **13** was not observed in *in vitro* and *in vivo* experiments. The K_d value of compound **13** was 2.90 ± 0.83 nM and its cell uptake was $1.32 \pm 0.10\%$ IA/ 10^6 cells (*in vitro*) and $7.87 \pm 2.37\%$ ID/g (*ex vivo*) on 22Rv1 tumor cells.^[51] In a pilot clinical study, PET/CT imaging was implemented in patients with metastasized PCa. All lesions were visualized and expressed in higher contrast images at 2 h p.i., than at 1 h, suggesting that imaging at a later time-point could be a better choice in this case. Compound **13** was the first compound to progress to a clinical trial because none of the other Al^{18}F -labeled PSMA agents has been examined in a clinical study.

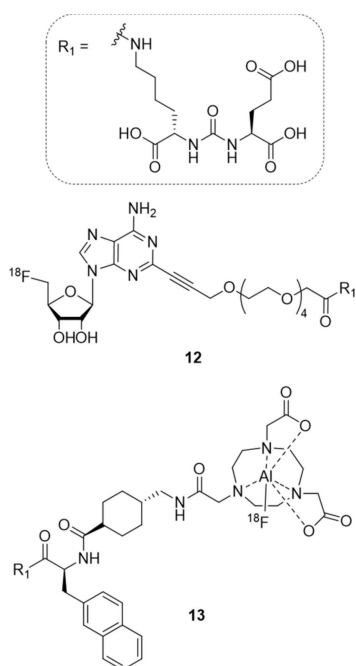


Figure 4. ^{18}F -labeled PSMA radioligands by other methods

Saji and co-workers designed novel PSMA-targeted succinimidyl-4-fluorobenzoate (SFB) compounds^[53] based on previous reports.^[54] In structure-activity relationship studies^[55], they found that high PSMA-binding affinity in this series was associated with the aromatic ring and the succinimidyl ring as linker moieties. On the other hand, PSMA-binding affinity was not influenced by the length of the linker between aromatic ring and succinimidyl moiety. The ^{18}F -SFB compounds (**14**–**15**, Figure 5) were synthesized in high decay-corrected radiochemical

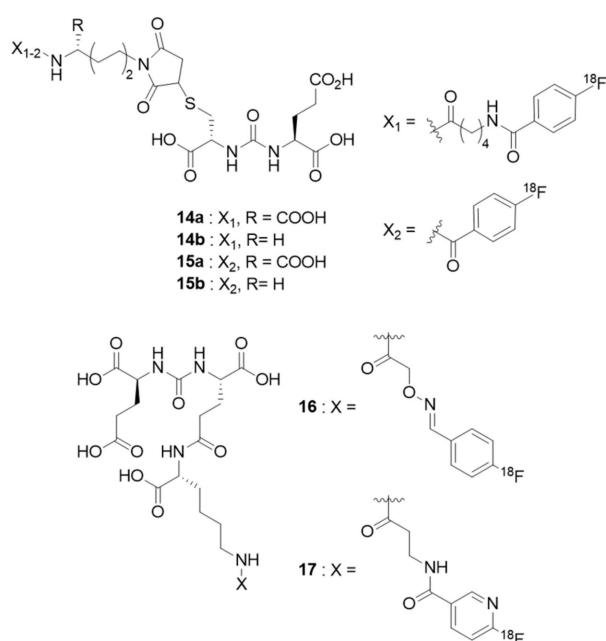


Figure 5. ^{18}F -labeled radiotracers with modified PSMA binding motif

yields of 30–50%, which is higher than that of **1** (synthetic radiochemical yield: 23%).^[56] *In vitro* binding inhibition assay showed that **14a**–**14b**, and **15a** had higher PSMA-binding affinity than **1** (K_i = 3.35 nM for **14a**, 8.69 nM for **14b**, 2.23 nM for **15a**, 15.5 nM for **1**). Additionally, **15a** exhibited LNCaP tumor accumulation similar to **1** at 60 min post-injection ($14.0 \pm 3.1\% \text{ID/g}$ for **15a**, $16.0 \pm 2.9\% \text{ID/g}$ for **1**) and tumor-to-liver ratio (4.8:1 for **15a**, 4.3:1 for **1**). Tumor-to-liver ratio is an important factor for PCa imaging because PCa are likely to metastasize to the pelvic and abdominal cavities.^[57] The ^{18}F -SFB compounds other than **15a** showed a lower LNCaP-to-liver ratio; therefore, **15a** could be a promising agent in this series.

There have been attempts to replace the Lys moiety of Lys-urea-Glu analogs with glutamic acid.^[58] Glu-urea-Glu ligands (**16**–**17**) also showed good PSMA targeting properties.^[59] Chemo-selective oxime ligation and acylation chemistry with ^{18}F -FPyl-TFP was applied to radiolabeling of **16** and **17**, respectively. Both **16** and **17** showed high radiochemical yields ($67 \pm 7\%$ and $53 \pm 7\%$, decay-corrected) and high PSMA-binding affinity (IC_{50} = 4.2 ± 0.4 nM for **16**, 1.1 ± 0.2 nM for **17**). Non-specific uptake in non-target tissue was rarely observed due to high hydrophilicity of **16** and **17**.

4. PSMA Radiotracers Modified with Diverse Linker or Chelator Group

Compound **2** was rapidly applied in clinical practice and became the most commonly used PSMA-targeting PET tracer.^[60] However, the chelator moiety of **2** forms relatively unstable complexes with trivalent therapeutic radionuclides including ^{177}Lu , ^{90}Y and ^{225}Ac . The HBED-CC chelator of **2** was simply replaced with DOTA, but this led to decreased tumor-targeting activities.^[16] Therefore, favorable pharmacokinetic and tumor-targeting properties of DOTA-conjugated compounds were achieved in combination with linker modification.

In general, potent PSMA ligands interact with Zn^{2+} ions, basic amino acids, Arg 210 and Lys 699, in $\text{S1}'$ subpocket, and lipophilic and π -cationic interactions at S1 subpocket. In addition, the interaction between the linker and the tunnel region of PSMA active site affects the pharmacokinetic properties as well as the additional PSMA-binding affinity. Relatively short-length linkers and nonpolar functionalities in the entrance region of the tunnel resulted in enhanced PSMA-binding affinity.^[41,61]

Eder and co-workers synthesized DOTA-conjugated PSMA inhibitors with various linker moieties and established structure-activity relationship.^[62] Compounds **18**–**23** (Figure 6) demonstrated that the aromatic moiety is important between Lys-urea-Glu and DOTA moiety. Among them, compound **21** which has three aromatic rings in the linker showed the most favorable K_i , cell surface binding, and specific internalization values in *in vitro* studies with LNCaP cells (K_i : 0.53 ± 0.47 nM, cell surface binding: $21.43 \pm 2.27\% \text{ IA}/10^6$ cells, specific internalization: $12.49 \pm 1.38\% \text{ IA}/10^6$ cells). In the set consisting of **3a** and **24**–**26**, at least one aromatic moiety with a rigid

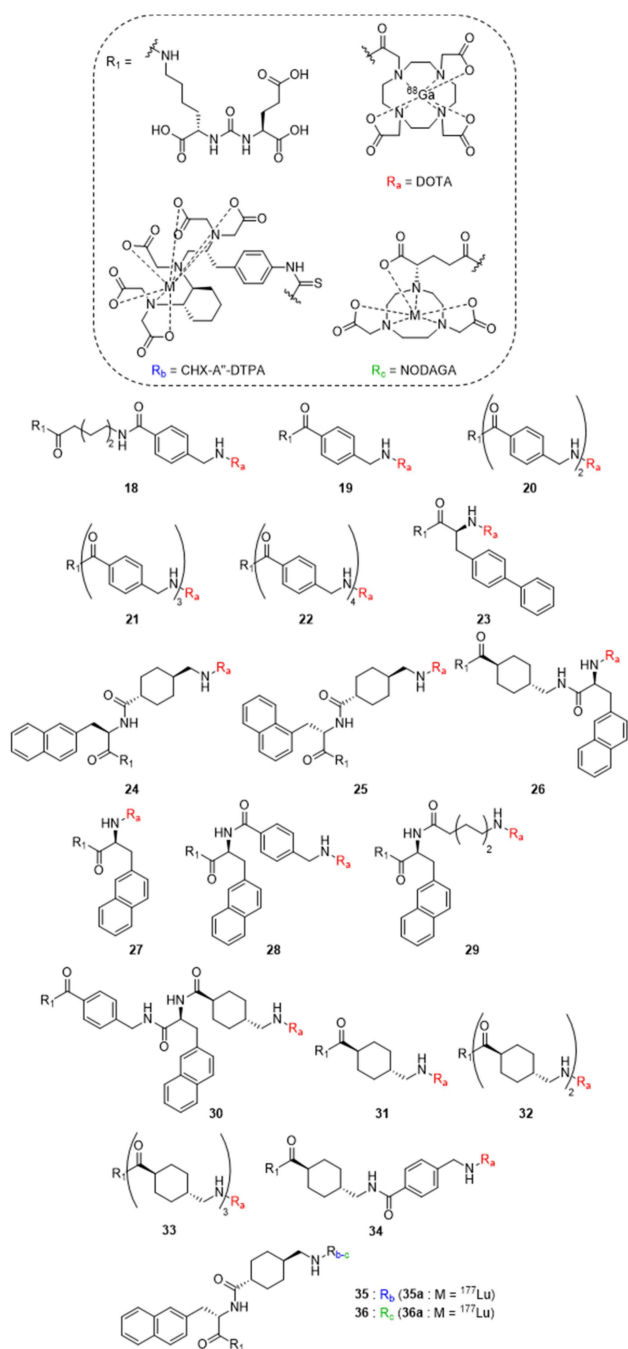


Figure 6. Linker- or chelator-modified PSMA ligands based on compound 3

conformation was critical for binding to PSMA. The deterioration of *in vitro* binding affinity and cell internalization was observed with chirality change (24) or reversed linker (26). (K_i : 8.86 ± 3.64 nM for 24, 17.70 ± 1.41 nM for 26). When the 1-naphthyl group was introduced instead of the 2-naphthyl group, steric hinderance occurred in the PSMA binding pocket and a decreased binding affinity was observed (K_i : 12.78 ± 6.41 nM for 25). In a set of compounds 27–30 functionalized with the 2-naphthyl-L-alanine structure, compound 28 with benzene ring instead of cyclohexane ring of 3 showed higher inhibitory activity (K_i : 1.81 ± 0.80 nM) than the others. However,

it exhibited decreased washout of radioactivity from the kidney as compared to 3a. The sole existence of cyclohexane moiety in the linkers of the last set of compounds, 31–34, did not contribute to PSMA binding affinity and cell internalization.

While maintaining the linker structure of compound 3, Mier and his colleagues studied the effect of chelator moiety on its pharmacokinetic properties.^[63] Compounds 35a and 36a (Figure 6) displayed higher internalization ($65.4 \pm 5.7\%$ for 35a and $48.5 \pm 16.4\%$ for 36a) than 2 ($17.9 \pm 0.7\%$) and 3b ($15.5 \pm 7.5\%$).

Since NOTA has been found to chelate ${}^{68}\text{Ga}$ more effectively than DOTA^[64], diverse efforts have been made to introduce NOTA into the chelator region of PSMA-targeted ligands. ${}^{68}\text{Ga}$ -labeled DOTA- and NOTA-chelated radiotracers (37, 38, Figure 7) with linker modification were designed and synthesized by Pomper group.^[65] The NOTA analog 38 showed higher PSMA-positive tumor uptake ($42.2 \pm 6.7\%$ ID/g at 1 h p.i.) and PIP/flu tumor uptake ratio (232 ± 26 at 2 h) than the DOTA analog, 37. ${}^{68}\text{Ga}$ -labeled PSMA ligands conjugated with DOTA or NOTA and a short linker (39, 40, Figure 7) were synthesized by Jeong and his colleagues with a kit formulation.^[66] They

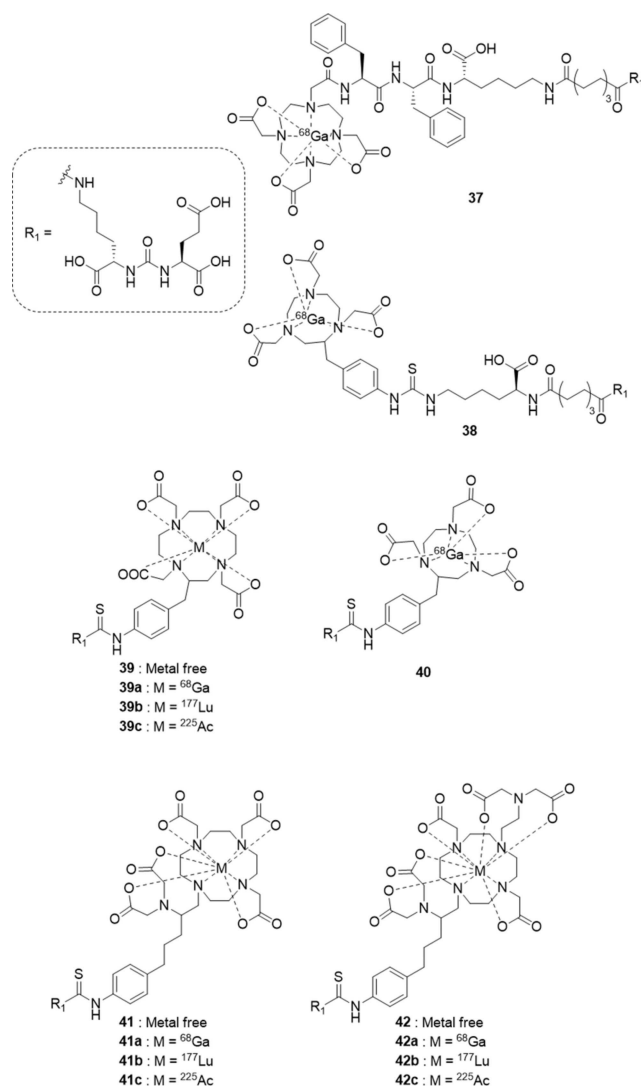


Figure 7. PSMA radioligands with various linker and chelator groups

developed a thiourea linker to improve the drawbacks of long-length linker including long synthetic step and low solubility problem. Compound **40** was labeled with ^{68}Ga with 99% efficiency at room temperature. It exhibited higher stability than **39a** in human serum for 2 h at 37 °C (8% free ^{68}Ga for **39a**, 1% free ^{68}Ga for **40**). Compounds **39a** and **40** revealed comparable tumor uptake (4.66 and 5.40%ID/g, respectively) to **2** (6.5%ID/g).

PSMA ligands functionalized with α -particle-emitting radionuclide (e.g., ^{225}Ac) have been considered as a useful radiopharmaceutical therapy modality of prostate cancer.^[25a,67] However, significant dissociation of ^{225}Ac -DOTA complex and side effects induced by free ^{225}Ac has been reported.^[68] Babich and co-workers synthesized and compared three compounds conjugated with octadentate (**39**, Figure 7), decadentate (**41**), and dodecadentate (**42**) chelating moieties.^[69] The IC_{50} values of metal-free **39** (13.3 ± 0.9 nM) and **41** (18.0 ± 3.7 nM) were comparable with that of **3** (12.2 ± 4.6 nM).^[63] However, the binding affinity of **42** was relatively weak (42.6 ± 6.6 nM). Although the ^{68}Ga chelating abilities of **39a**, **41a**, **42a** were similar, the chelation yields of ^{177}Lu and ^{225}Ac changed dramatically. For example, **41b** exhibited 65.2 \pm 15.4% chelation yield after 30 min at 25 °C, despite that the chelation yields of **39b** and **42b** were less than 10% at 25 °C.

5. Multivalency Ligands

Multivalent interactions can generally be stronger even though monovalent interactions are weak. Furthermore, multivalency increases the selectivity of a ligand for a receptor. Multivalent ligands targeting PSMA have been developed to enhance PSMA-binding affinity *in vitro* and to improve the accuracy of dosimetry *in vivo*. Notni and co-workers reported a dendritic molecule (**43** in Figure 8) employing four TRAP (1,1,4,7-triazacyclononane-1,4,7-tris[methylene(2-carboxyethyl)-phosphonic acid]) motif^[70] with hexameric PSMA-targeting Lys-urea-Glu moiety.^[71] The efficiency of ^{68}Ga incorporation on tetra-TRAP dendrimer was 10-fold higher than that on monomeric TRAP.^[70] In competitive displacement assays with LNCaP cells, compound **43** showed excellent PSMA binding affinity (IC_{50} of 1.2 ± 0.2 nM) accentuating the multimerization effect in relation to the optimized Lys-urea-Glu monomer.^[16,62] High hydrophilicity ($\text{Log } D = -4.4 \pm 0.1$ at pH 7.4) of **43** resulted in rapid renal clearance. The same research group also endeavored to establish dual-radionuclide labeled radiopharmaceuticals.^[72] They used the orthogonal metal ion selectivity of polyphosphinate chelator DOTPI (1,4,7,10-tetraazacyclododecane-1,4,7,10-tetrakis[methylene(2-carboxyethyl)phosphonic acid]), for large trivalent cations including Bi^{3+} ^[73] and TRAP (for small trivalent cations, particularly Ga^{3+}) (**44a**, **45a** in Figure 8).^[74] They

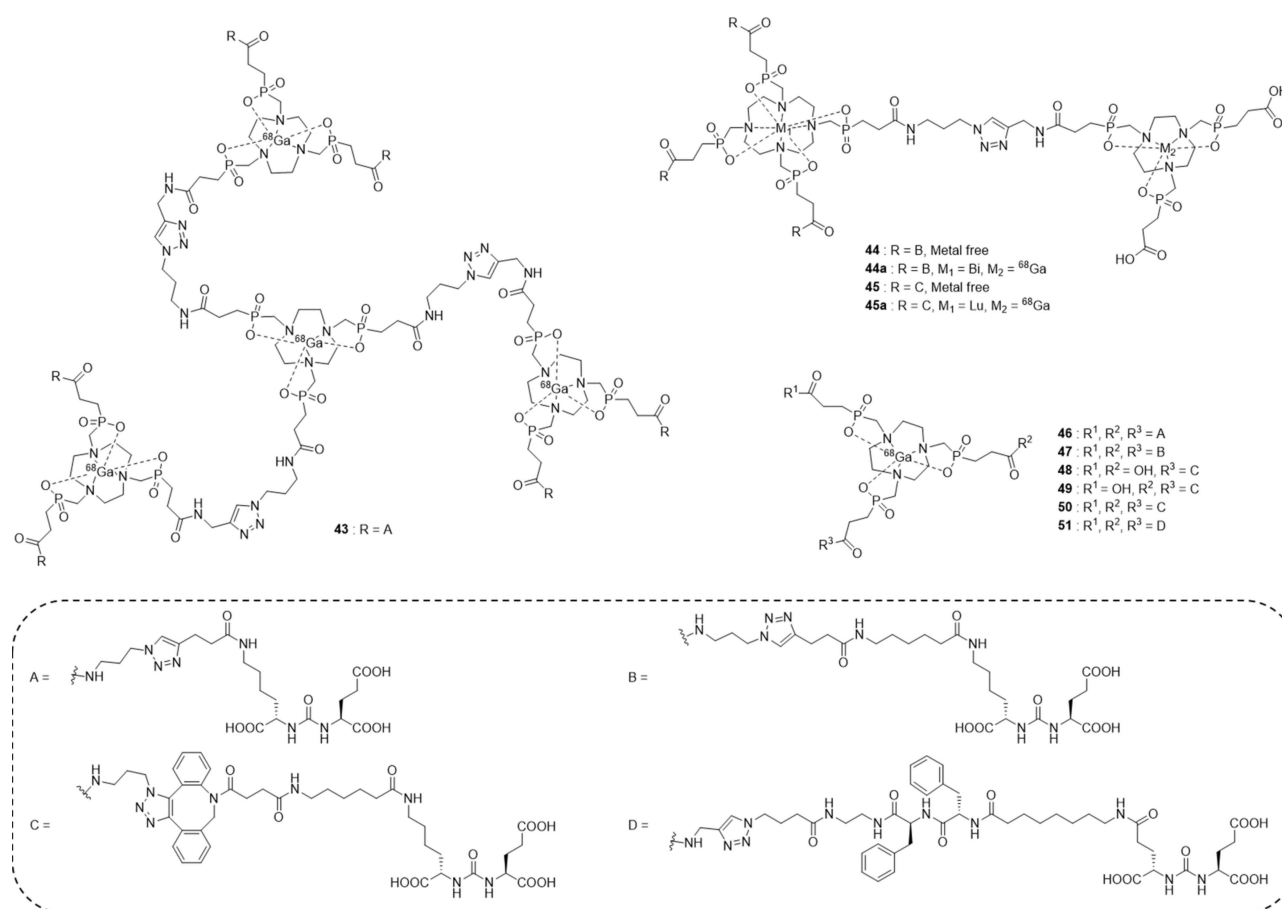


Figure 8. Homo-multivalent PSMA ligands

achieved $[Ga^{3+}(TRAP)]$ and $[M^{3+}(DOTPI)]$ complexation selectively. Because both $[M^{3+}(TRAP)]^{[75]}$ and $[Ga^{3+}(DOTPI)]^{[73]}$ are not inert kinetically, transchelation with Na_3DTPA or Na_2EDTA could eliminate the unstable forms. PSMA binding affinities of unlabeled **44** and **45** were 2.5 ± 0.2 nM and 2.8 ± 0.3 nM, respectively.

Based on TRAP scaffold, compounds **46–47** were obtained by Cu(I)-mediated Huisgen coupling (CuAAC) while compounds **48–50** were done by DBCO (dibenzocyclooctyne)-based SPAAC (strain-promoted alkyne-azide cycloadditions).^[76] The compounds were compared with the trimer PSMA ligand, **51**. All six compounds (**46–51**) exhibited nanomolar IC_{50} values supporting the affinity enhancement of trimerization.^[77]

The selectivity and retention in tumor tissues that over-express PSMA and other receptors can be synergistically increased by applying a dual-targeting strategy. In order to improve sensitivity and specificity for PSMA-expressing tumors, several heteromultivalent agents that have a wide range of phenotypes have been investigated.^[78] Pomper group reported heterobivalent (HtBv) ligands targeting integrin- $\alpha_v\beta_3$, a family of transmembrane proteins dysregulated in diverse cancer, in combination with PSMA.^[79] Approximately 20 Å in length of linker is required to deliver PSMA-targeting Lys-urea-Glu scaffold to the PSMA-binding site^[80], while Lys was a suitable linker length between integrin- $\alpha_v\beta_3$ interface and imaging moiety.^[81] β -glutamic acid as a linker was exploited for the

purpose of conjugating a PSMA-targeting Lys-urea-Glu motif, an integrin-targeting cRGDfK motif, and an optical-dye SulfoCy7. The HtBv ligand (**52** in Figure 9) has similar PSMA-affinity for PSMA as compared with DOTA-conjugated monovalent compound. Compound **52** also exhibited strong integrin- $\alpha_v\beta_3$ binding affinity ($IC_{50} = 90$ nM) comparable to that of cRGDfK-DOTA conjugate ($IC_{50} = 74$ nM). Synergistic dual targeting specificity were demonstrated with SulfoCy7-labeled **53** (Figure 9) in the *in vivo* optical imaging of NOD/SCID mice bearing integrin/PSMA-positive tumors.

Byun and co-workers developed the HtBv ligand (**54** in Figure 9) targeting PSMA with hepsin, a type II transmembrane serine protease which is highly expressed on the epithelial cell surface of PCa.^[82] Cell uptake studies using PC3/ML-PSMA (PSMA expressing cell line), PC3/ML-HPN (hepsin expressing cell line), and PC3/ML-PSMA-HPN (PSMA and hepsin expressing cell line) demonstrated synergistic affinity enhancement of **54**.

Chen and his colleagues attempted to increase the blood circulation half-life of PSMA-targeted agents to improve tumor uptake for therapeutic or imaging efficacy.^[83] They attached Evans Blue (**55** in Figure 9) or 4-(*p*-iodophenyl)butyric acid (**56** in Figure 9) as albumin-binding moieties.^[84] The IC_{50} values of **55** and **56** were 13.7 and 30.1 nM, respectively. The slow blood clearance of **55 a** ($t_{1/2} = 5.6$ h) contributed to the maintained tumor uptake of **55 a** at 24 hr and 48 hr p.i. ($74.5 \pm 11.0\%$ ID/g

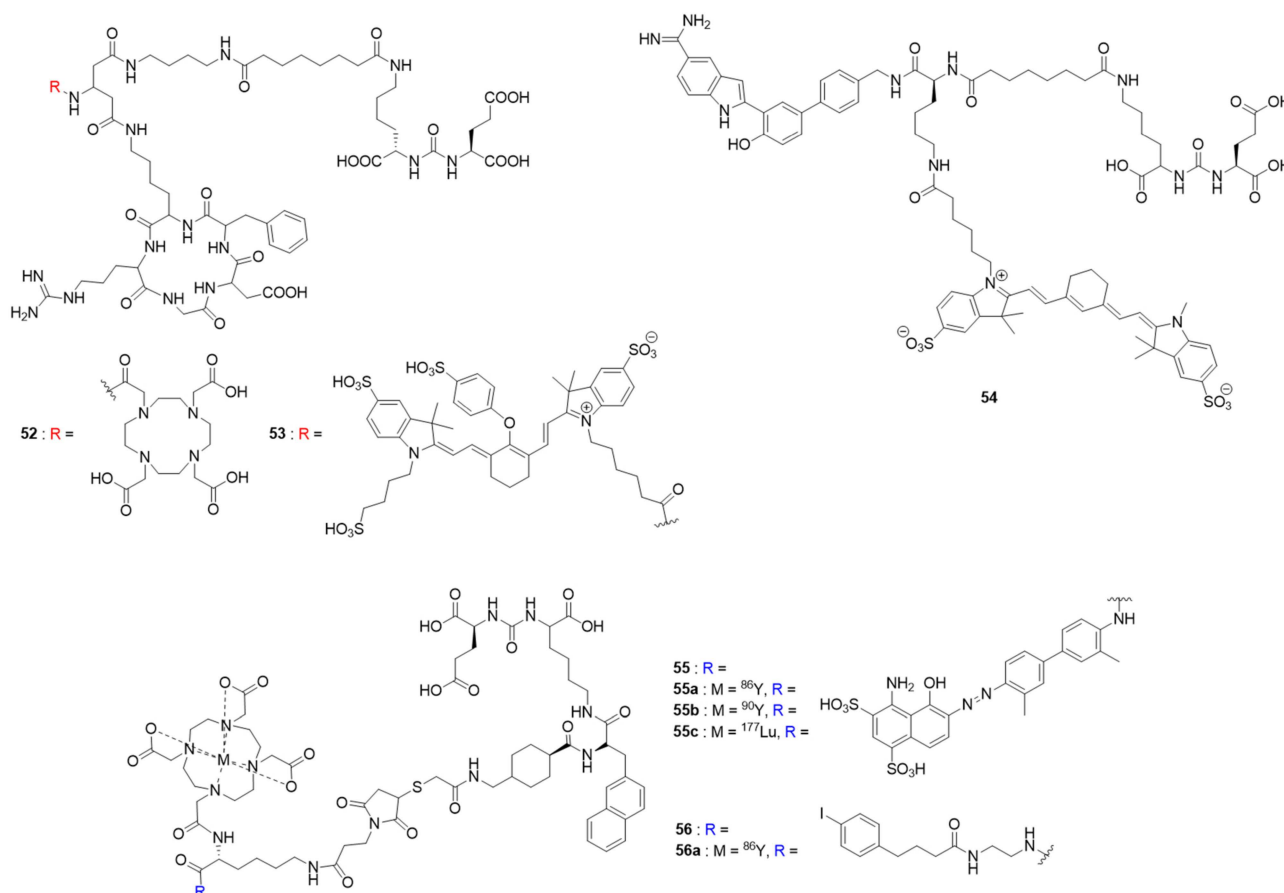


Figure 9. Heterobivalent ligands targeting in PSMA and other proteins.

and $77.3 \pm 6.2\%$ ID/g, respectively) while tumor uptake of **56a** decreased over time.

6. Multi-Functional Ligands

The radiolabeled PSMA-targeting agents have corroborated accurate images of PCa specifically by radionuclide imaging such as PET and SPECT. However, a greater resolution would be required for the visualization of fine tumor margins during surgical operation.^[85] Recent studies have reported simultaneous fluorescence (FL) and SPECT or PET visualization at the same time.^[86] Introduction of FL and PET modalities on the same ligand can be adopted to avoid the limitations associated with the pharmacokinetics of stand-alone FL or PET agents. It should be noted that radioactive specificity may be compromised due to the higher detection threshold for FL than PET or SPECT. Ting and co-workers designed and synthesized the dual-imaging agent (**57** in Figure 10) for FL and PET scanning.^[87] They used cyanine moiety as fluorophore and

alkylammoniomethyl trifluoroborate (AMBF₃) as ¹⁸F-captor.^[88] The AMBF₃ moiety contributed to rapid and stable exchange with ¹⁸F in aqueous environment. Compound **57** exhibited IC₅₀ value of 6.74 ± 1.33 nM and revealed a high radiochemical yield (14–31%, decay uncorrected). Compound **57** displayed PSMA specificity with 5.2-fold higher fluorescent signal in PSMA-positive PIP cells than in PSMA-negative PC3 cells.

Sun and co-workers synthesized theranostic small molecule-drug conjugates.^[89] Compound **58** has both PET-imaging and chemotherapy moieties. By utilizing the three attachment points of Lys, a NOTA moiety for chelating ⁶⁸Ga, a cytotoxic maytansinoid emtansine (DM1) for chemotherapy was linked to the Lys-Urea-Glu scaffold. DM1 has been applied in targeted therapy, for instance, antibody-drug conjugate.^[90] ⁶⁸Ga-radio-labeling of **58** was conducted at 60 °C and showed quantitative yield in 15 min with 50–80 Gbq/μmol of specific activity range. In an *in vitro* PSMA binding affinity assay, **58** had IC₅₀ values of 187 ± 41 nM. Clear PET/CT image of **58** in xenografted SCID mice was visualized at 1 h p.i. with $4.30 \pm 0.20\%$ ID/g of tumor uptake. The radioactivity accumulated in the liver was very low ($0.42 \pm 0.10\%$ ID/g), implying the reduction of systemic toxicity of DM1.

The antibody-recruiting small molecule approaches conjugating PSMA-targeted moiety with 2,4-dinitrophenyl (DNP) group as the immune cell promoting scaffold were recently reported.^[91] Valliant and co-workers reported PSMA-binding DNP derivatives (**59–63** in Figure 10) radiolabeled with ¹²⁵I for SPECT-imaging.^[92] The *in vitro* assay with LNCaP cells revealed that the 5-iodotriazole derivative, **63**, had the most potent affinity (IC₅₀ = 14 nM) in this series. The 4-iodotriazole derivative with no PEG linker had an IC₅₀ value of 100 nM, while that of the DNP derivative (**59**) was 3 nM, implying the significance of the arene-binding region.

7. New Scaffolds to Replace PSMA-Binding Lys-urea-Glu Moiety

Pomper and his colleagues synthesized PSMA inhibitors based on carbamate scaffold to decrease the uptake into non-target organ.^[93] Although the substituted O for NH weakened the hydrogen-bonding interactions presented by the urea functional group, the carbamate-based compounds (**64–65** in Figure 10) maintained the overall geometry and interactions with the Arg patch region and S1 hydrophobic subpocket compared to their urea analogs **66** and **67**.^[41] Compounds **64–65** exhibited strong PSMA binding affinities ($K_i = 0.11$ nM for **64**, 0.21 for **65**) which were higher than that of **1** ($K_i = 1.1$ nM). They also exhibited excellent selective PSMA-positive PC3 PIP tumor uptake (**64**: 90% ID/g at 2 h; **65**: 97% ID/g at 4 h), and radioactivity in non-target organs cleared rapidly. Tsukamoto and co-workers supported the promising perspective of the carbamate scaffold with structure-activity relationship studies.^[94]

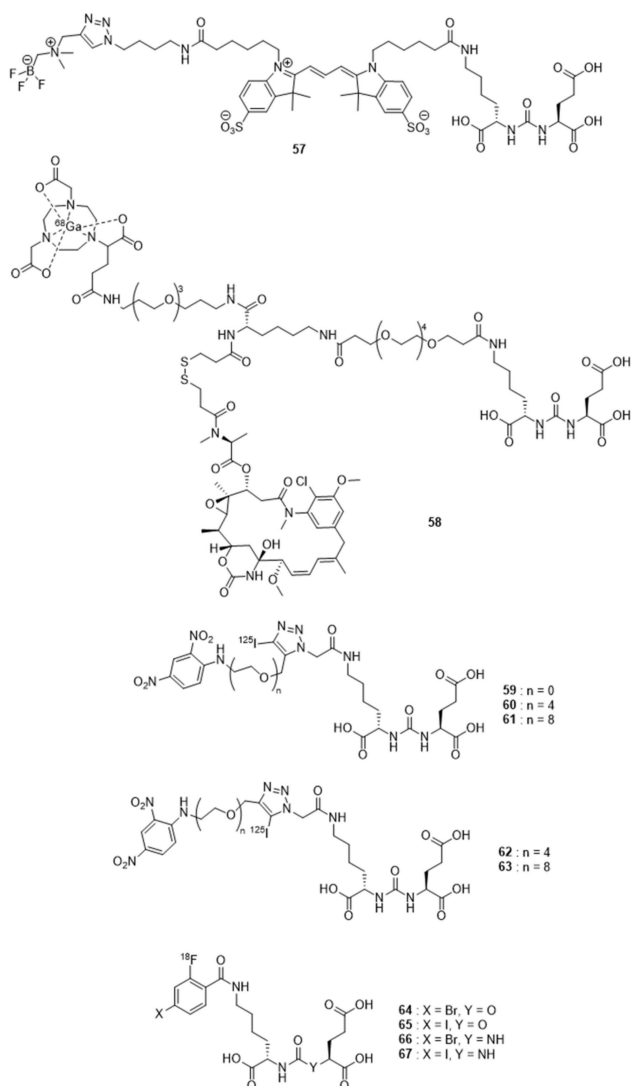


Figure 10. Multifunctional or new scaffold bearing PSMA ligands

8. Outlook

Table 1 summarizes the PSMA-binding affinity, tumor uptake, signal-to-noise (S/N) ratio and radiochemical yield of the representative compounds described in this review. PSMA-targeted tracers (1–3) in clinical stage for prostate cancer imaging have strong IC_{50} values (< 30 nM), high tumor uptake (> 7 %ID/g), and high S/N ratio (> 7). This value is not essential for the success of radiolabeled PSMA molecules, but can be used as a guideline in preclinical studies. As the S1 subpocket of PSMA is highly resistant for structural changes and the tunnel region is sufficiently flexible to accommodate bulky linkers and prosthetic groups, it is expected that structural modification of Lys-urea-Glu PSMA inhibitors would continue in the P1 region and the tunnel region.

Despite the promising clinical results of radiolabeled PSMA ligands, there is still a clinical need to maximize the efficiency of diagnosis or treatment and to minimize the side effect. In particular, potential toxicities such as hematotoxicity and xerostomia should be considered and adequately assessed.

Table 1. Biological data summary of representative PSMA inhibitors

Cmpd.	PSMA affinity [nM]	Tumor uptake [%ID/g]	S/N ratio	Radiochemical yield	Ref.
1	1.1 ^{a,d} , 15.5 ^{b,c}	46.7 ± 5.8 (0.5 h)	184 (1 h) ^g	36–53% ^e 2.8% ^f	[11,33,53]
2	7.5 ^{b,d} , 24.3 ^{b,c}	7.7 ± 1.5 (1 h)	13 (1 h) ^g	> 99%	[16,63,66]
3	6.4 ^{a,c}	8.5 ± 4.1 (1 h)	7.8 (1 h) ^g	> 97%	[22]
5	6.7 ^{a,c}	8.0 ± 2.4 (1 h)	13 (1 h) ^g	5–10% ^f	[35]
6	12.9 ^{a,d}	40.3 ± 5.1 (0.5 h)	302 (2 h) ^g	14% ^f	[39]
9b	7.0 ^{b,c}	14.3 ± 2.5 (2 h)		20–40% ^e	[32]
9c	3.2 ^{b,c}	10.9 ± 1.0 (2 h)		20–40% ^e	[32]
13	2.9 ^{a,c}	7.9 ± 2.4 (0.5 h)	65 (1.5 h) ^h	32% ^f	[51]
14a	3.4 ^{a,c}	13.3 ± 2.2 (1 h)	33 (1 h) ^g	30–50% ^e	[53]
14b	8.7 ^{a,c}	7.2 ± 2.1 (1 h)	24 (1 h) ^g	30–50% ^e	[53]
15a	2.2 ^{a,c}	14.0 ± 3.1 (1 h)	18 (1 h) ^g	30–50% ^e	[53]
15b	17.6 ^{b,c}	7.7 ± 1.4 (1 h)	11 (1 h) ^g	30–50% ^e	[53]
37	0.3 ^{a,d}	19.5 ± 1.8 (1 h)	59 (1 h) ^g	-	[65]
38	0.4 ^{a,d}	42.2 ± 6.7 (1 h)	120 (1 h) ^g	-	[65]
40	18.3 ^{b,c}	5.4 ± 0.4 (1 h)	32 (1 h) ^g	-	[66]
44	2.5 ^{b,c}	2.8 ± 0.3 (1 h)	22 (1 h) ^h	-	[72]
45	2.8 ^{b,c}	3.3 ± 0.3 (1 h)	17 (1 h) ^h	-	[72]
46	6.0 ^{b,c}	1.2 ± 0.5 (1 h)	17 (1 h) ^h	-	[76]
47	1.5 ^{b,c}	4.2 ± 0.9 (1 h)	42 (1 h) ^h	-	[76]
48	1.4 ^{b,c}	2.6 ± 0.6 (1 h)	7.1 (1 h) ^h	-	[76]
49	2.1 ^{b,c}	3.3 ± 0.6 (1 h)	11 (1 h) ^h	-	[76]
50	2.5 ^{b,c}	3.0 ± 0.1 (1 h)	14 (1 h) ^h	-	[76]
51	2.0 ^{b,c}	4.0 ± 0.1 (1 h)	11 (1 h) ^h	-	[76]
58	187 ^{b,c}	4.3 ± 0.2 (1 h)	-	-	[89]
59	3 ^{b,c}	12.2 ± 1.9 (1 h)	35 (1 h) ^g	72% ^e	[92]
63	14 ^{b,c}	3.0 ± 0.2 (1 h)	10 (1 h) ^g	70% ^e	[92]
64	0.1 ^{a,d}	64.5 ± 7.7 (1 h)	40 (1 h) ^g	5% ^f	[93]
65	0.2 ^{a,d}	57.1 ± 19.6 (1 h)	20 (1 h) ^g	3% ^f	[93]

a) K_i value; b) IC_{50} value; c) cell binding assay; d) enzymatic assay; e) decay-corrected; f) nondecay-corrected; g) tumor-to-blood ratio; h) tumor-to-muscle ratio

9. Conclusion

PSMA is now considered as an excellent biomarker for metastatic prostate cancer. SARs of urea-based PSMA ligands derived from Lys-urea-Glu have been extensively established in the last decade. Preclinical and clinical studies using PSMA-targeting ligands have been actively performed.

Radiotherapy using β - or α -emitting PSMA-targeted ligands showed bright prospect for the treatment of recurrent PCa. In particular, ^{225}Ac -labeled compounds with strong efficacy and long half-life need to be validated in clinical trials to assess the benefits of PSMA-targeted radiotherapy in comparison with other standard therapies of prostate cancer.

Significant progress and clinical achievement of prostate cancer imaging with radiolabeled compounds 1–3 have been made. They have a potential to be approved by FDA as the PSMA-targeted low molecular weight imaging probe if the associated problems including non-target organ uptake, low radiochemical yield, unstable complexation with radiometals, and pharmacokinetic properties are resolved.

Acknowledgements

We acknowledge the supports from the National Research Foundation (2017R1A2B4005036 and 2019R1A6A1A03031807) and Ministry of Health & Welfare, Republic of Korea (HI16C1827).

Conflict of Interest

The authors declare no conflict of interest.

Keywords: Prostate cancer · PSMA · imaging agents · radionuclide · radiotherapy

- [1] R. L. Siegel, K. D. Miller, A. Jemal, *Ca-Cancer J. Clin.* **2018**, *68*, 7–30.
- [2] A. J. Chang, K. A. Autio, M. Roach 3rd, H. I. Scher, *Nat. Rev. Clin. Oncol.* **2014**, *11*, 308–323.
- [3] R. M. Hoffman, *N. Engl. J. Med.* **2011**, *365*, 2013–2019.
- [4] a) A. Ghosh, W. D. Heston, *J. Cell. Biochem.* **2004**, *91*, 528–539; b) D. A. Silver, I. Pellicer, W. R. Fair, W. D. Heston, C. Cordon-Cardo, *Clin. Cancer Res.* **1997**, *3*, 81–85.
- [5] a) D. G. Bostwick, A. Pacelli, M. Blute, P. Roche, G. P. Murphy, *Cancer* **1998**, *82*, 2256–2261; b) S. S. Chang, *Rev. Urol.* **2004**, *6*, S13–S18.
- [6] a) S. A. Rajasekaran, G. Anilkumar, E. Oshima, J. U. Bowie, H. Liu, W. Heston, N. H. Bander, A. K. Rajasekaran, *Mol. Biol. Cell* **2003**, *14*, 4835–4845; b) J. S. Ross, C. E. Sheehan, H. A. Fisher, R. P. Kaufman, Jr., P. Kaur, K. Gray, I. Webb, G. S. Gray, R. Mosher, B. V. Kallakury, *Clin. Cancer Res.* **2003**, *9*, 6357–6362.
- [7] a) N. H. Bander, *Nat. Clin. Pract. Urol.* **2006**, *3*, 216–225; b) R. J. Barren, 3rd, E. H. Holmes, A. L. Boynton, S. L. Misrock, G. P. Murphy, *The Prostate* **1997**, *30*, 65–68.
- [8] A. P. Kozikowski, F. Nan, P. Conti, J. Zhang, E. Ramadan, T. Bzdega, B. Wroblewska, J. H. Neale, S. Pshenichkin, J. T. Wroblewski, *J. Med. Chem.* **2001**, *44*, 298–301.
- [9] C. A. Foss, R. C. Mease, S. Y. Cho, H. J. Kim, M. G. Pomper, *Curr. Med. Chem.* **2012**, *19*, 1346–1359.
- [10] a) M. G. Pomper, J. L. Musachio, J. Zhang, U. Scheffel, Y. Zhou, J. Hilton, A. Maini, R. F. Dannals, D. F. Wong, A. P. Kozikowski, *Mol. Imaging* **2002**, *1*, 96–101; b) R. C. Mease, C. L. Dusich, C. A. Foss, H. T. Ravert, R. F.

- Dannals, J. Seidel, A. Prideaux, J. J. Fox, G. Sgouros, A. P. Kozikowski, M. G. Pomper, *Clin. Cancer Res.* **2008**, *14*, 3036–3043.
- [11] Y. Chen, M. Pullambhatla, C. A. Foss, Y. Byun, S. Nimmagadda, S. Senthambhichelvan, G. Sgouros, R. C. Mease, M. G. Pomper, *Clin. Cancer Res.* **2011**, *17*, 7645–7653.
- [12] G. Bauman, P. Martin, J. D. Thiessen, R. Taylor, M. Moussa, M. Gaed, I. Rachinsky, Z. Kassam, J. Chin, S. Pautler, T. Y. Lee, J. F. Valliant, A. Ward, *Eur. Urol. Focus* **2018**, *4*, 702–706.
- [13] M. A. Gorin, S. P. Rowe, H. D. Patel, I. Vidal, M. Mana-Ay, M. S. Javadi, L. B. Solnes, A. E. Ross, E. M. Schaeffer, T. J. Bivalacqua, A. W. Partin, K. J. Pienta, Z. Szabo, A. M. De Marzo, M. G. Pomper, M. E. Allaf, *J. Urol.* **2018**, *199*, 126–132.
- [14] A. Sanchez-Crespo, P. Andreo, S. A. Larsson, *Eur. J. Nucl. Med. Mol. Imaging* **2004**, *31*, 44–51.
- [15] S. R. Banerjee, M. Pullambhatla, Y. Byun, S. Nimmagadda, G. Green, J. J. Fox, A. Horti, R. C. Mease, M. G. Pomper, *J. Med. Chem.* **2010**, *53*, 5333–5341.
- [16] M. Eder, M. Schafer, U. Bauder-Wust, W. E. Hull, C. Wangler, W. Mier, U. Haberkorn, M. Eisenhut, *Bioconjugate Chem.* **2012**, *23*, 688–697.
- [17] J. J. Morigi, P. D. Stricker, P. J. van Leeuwen, R. Tang, B. Ho, Q. Nguyen, G. Hruby, G. Fogarty, R. Jagavkar, A. Kneebone, A. Hickey, S. Fanti, L. Tarlinton, L. Emmett, *J. Nucl. Med.* **2015**, *56*, 1185–1190.
- [18] A. Afshar-Oromieh, E. Avtzi, F. L. Giesel, T. Holland-Letz, H. G. Linhart, M. Eder, M. Eisenhut, S. Boxler, B. A. Hadaschik, C. Kratochwil, W. Weichert, K. Kopka, J. Debus, U. Haberkorn, *Eur. J. Nucl. Med. Mol. Imaging* **2015**, *42*, 197–209.
- [19] F. Ceci, P. Castellucci, T. Graziani, A. Farolfi, C. Fonti, F. Lodi, S. Fanti, *Eur. J. Nucl. Med. Mol. Imaging* **2019**, *46*, 31–39.
- [20] M. McCarthy, R. Francis, C. Tang, J. Watts, A. Campbell, *Int. J. Radiat. Oncol. Biol. Phys.* **2019**.
- [21] P. J. van Leeuwen, L. Emmett, B. Ho, W. Delprado, F. Ting, Q. Nguyen, P. D. Stricker, *BJU Int.* **2017**, *119*, 209–215.
- [22] M. Benesova, M. Schafer, U. Bauder-Wust, A. Afshar-Oromieh, C. Kratochwil, W. Mier, U. Haberkorn, K. Kopka, M. Eder, *J. Nucl. Med.* **2015**, *56*, 914–920.
- [23] K. Rahbar, H. Ahmadzadehfar, C. Kratochwil, U. Haberkorn, M. Schafers, M. Essler, R. P. Baum, H. R. Kulkarni, M. Schmidt, A. Drzezga, P. Bartenstein, A. Pfestroff, M. Luster, U. Lutzen, M. Marx, V. Prasad, W. Brenner, A. Heinzl, F. M. Mottaghy, J. Ruf, P. T. Meyer, M. Heuschkel, M. Eveslage, M. Bogemann, W. P. Fendler, B. J. Krause, *J. Nucl. Med.* **2017**, *58*, 85–90.
- [24] M. S. Hofman, J. Violet, R. J. Hicks, J. Ferdinandus, S. P. Thang, T. Akhurst, A. Irvani, G. Kong, A. Ravi Kumar, D. G. Murphy, P. Eu, P. Jackson, M. Scalzo, S. G. Williams, S. Sandhu, *Lancet Oncol.* **2018**, *19*, 825–833.
- [25] a) K. E. Baidoo, K. Yong, M. W. Brechbiel, *Clin. Cancer Res.* **2013**, *19*, 530–537; b) M. Miederer, D. A. Scheinberg, M. R. McDevitt, *Adv. Drug Delivery Rev.* **2008**, *60*, 1371–1382.
- [26] H. Liu, A. K. Rajasekaran, P. Moy, Y. Xia, S. Kim, V. Navarro, R. Rahmati, N. H. Bander, *Cancer Res.* **1998**, *58*, 4055–4060.
- [27] a) M. R. McDevitt, D. Ma, L. T. Lai, J. Simon, P. Borchardt, R. K. Frank, K. Wu, V. Pellegrini, M. J. Curcio, M. Miederer, N. H. Bander, D. A. Scheinberg, *Science* **2001**, *294*, 1537–1540; b) M. Miederer, G. Henriksen, A. Alke, I. Mossbrugger, L. Quintanilla-Martinez, R. Senekowitsch-Schmidtke, M. Essler, *Clin. Cancer Res.* **2008**, *14*, 3555–3561.
- [28] C. Kratochwil, F. Bruchertseifer, F. L. Giesel, M. Weis, F. A. Verburg, F. Mottaghy, K. Kopka, C. Apostolidis, U. Haberkorn, A. Morgenstern, *J. Nucl. Med.* **2016**, *57*, 1941–1944.
- [29] M. Sathekge, F. Bruchertseifer, O. Knoesen, F. Reyneke, I. Lawal, T. Lengana, C. Davis, J. Mahapane, C. Corbett, M. Vorster, A. Morgenstern, *Eur. J. Nucl. Med. Mol. Imaging* **2019**, *46*, 129–138.
- [30] M. Sathekge, O. Knoesen, M. Meckel, M. Modiselle, M. Vorster, S. Marx, *Eur. J. Nucl. Med. Mol. Imaging* **2017**, *44*, 1099–1100.
- [31] C. Kratochwil, K. Schmidt, A. Afshar-Oromieh, F. Bruchertseifer, H. Rathke, A. Morgenstern, U. Haberkorn, F. L. Giesel, *Eur. J. Nucl. Med. Mol. Imaging* **2018**, *45*, 31–37.
- [32] J. Kelly, A. Amor-Coarasa, A. Nikolopoulou, D. Kim, C. Williams, Jr., S. Ponnala, J. W. Babich, *Eur. J. Nucl. Med. Mol. Imaging* **2017**, *44*, 647–661.
- [33] Z. Szabo, E. Mena, S. P. Rowe, D. Plyku, R. Nidal, M. A. Eisenberger, E. S. Antonarakis, H. Fan, R. F. Dannals, Y. Chen, R. C. Mease, M. Vranesic, A. Bhatnagar, G. Sgouros, S. Y. Cho, M. G. Pomper, *Mol. Imaging Biol.* **2015**, *17*, 565–574.
- [34] B. D. Zlatopolskiy, H. Endepols, P. Krapf, M. Guliyev, E. A. Urusova, R. Richarz, M. Hohberg, M. Dietlein, A. E. Drzezga, B. Neumaier, *J. Nucl. Med.* **2018**.
- [35] J. Cardinale, M. Schafer, M. Benesova, U. Bauder-Wust, K. Leotta, M. Eder, O. C. Neels, U. Haberkorn, F. L. Giesel, K. Kopka, *J. Nucl. Med.* **2017**, *58*, 425–431.
- [36] F. L. Giesel, B. Hadaschik, J. Cardinale, J. Radtke, M. Vinsensia, W. Lehnert, C. Kesch, Y. Tolstov, S. Singer, N. Grabe, S. Duensing, M. Schafer, O. C. Neels, W. Mier, U. Haberkorn, K. Kopka, C. Kratochwil, *Eur. J. Nucl. Med. Mol. Imaging* **2017**, *44*, 678–688.
- [37] U. Kragh-Hansen, V. T. Chuang, M. Otagiri, *Biol. Pharm. Bull.* **2002**, *25*, 695–704.
- [38] F. L. Giesel, K. Knorr, F. Spohn, L. Will, T. Maurer, P. Flechsig, O. Neels, K. Schiller, H. Amaral, W. A. Weber, U. Haberkorn, M. Schwaiger, C. Kratochwil, P. Choyke, V. Kramer, K. Kopka, M. Eiber, *J. Nucl. Med.* **2019**, *60*, 362–368.
- [39] Y. Chen, A. Lisok, S. Chatterjee, B. Wharram, M. Pullambhatla, Y. Wang, G. Sgouros, R. C. Mease, M. G. Pomper, *Bioconjugate Chem.* **2016**, *27*, 1655–1662.
- [40] C. Mamat, T. Ramenda, F. R. Wuest, *Mini-Rev. Org. Chem.* **2009**, *6*, 21–34.
- [41] C. Barinka, Y. Byun, C. L. Dusich, S. R. Banerjee, Y. Chen, M. Castaneres, A. P. Kozikowski, R. C. Mease, M. G. Pomper, J. Lubkowski, *J. Med. Chem.* **2008**, *51*, 7737–7743.
- [42] A. E. Machulkin, Y. A. Ivanenkov, A. V. Aladinskaya, M. S. Veselov, V. A. Aladinskiy, E. K. Beloglazkina, V. E. Kotelianskiy, A. G. Shakhbazyan, Y. B. Sandulenko, A. G. Majouga, *J. Drug Targeting* **2016**, *24*, 679–693.
- [43] V. D. Bock, D. Speijer, H. Hiemstra, J. H. van Maarseveen, *Org. Biomol. Chem.* **2007**, *5*, 971–975.
- [44] J. Tykvart, J. Schimer, A. Jancarik, J. Barinkova, V. Navratil, J. Starkova, K. Sramkova, J. Konvalinka, P. Majer, P. Sacha, *J. Med. Chem.* **2015**, *58*, 4357–4363.
- [45] a) K. Lang, J. W. Chin, *ACS Chem. Biol.* **2014**, *9*, 16–20; b) J. P. Meyer, P. Adumeau, J. S. Lewis, B. M. Zeglis, *Bioconjugate Chem.* **2016**, *27*, 2791–2807; c) M. Meldal, C. W. Tornoe, *Chem. Rev.* **2008**, *108*, 2952–3015.
- [46] a) J. Gierlich, G. A. Burley, P. M. Gramlich, D. M. Hammond, T. Carell, *Org. Lett.* **2006**, *8*, 3639–3642; b) E. Lallana, E. Fernandez-Megia, R. Riguera, *J. Am. Chem. Soc.* **2009**, *131*, 5748–5750; c) A. J. Link, M. K. Vink, D. A. Tirrell, *J. Am. Chem. Soc.* **2004**, *126*, 10598–10602.
- [47] M. Wang, C. D. McNitt, H. Wang, X. Ma, S. M. Scarry, Z. Wu, V. V. Popik, Z. Li, *Chem. Commun.* **2018**, *54*, 7810–7813.
- [48] D. O'Hagan, C. Schaffrath, S. L. Cobb, J. T. Hamilton, C. D. Murphy, *Nature* **2002**, *416*, 279.
- [49] P. T. Lowe, S. Dall'Angelo, I. N. Fleming, M. Piras, M. Zanda, D. O'Hagan, *Org. Biomol. Chem.* **2019**, *17*, 1480–1486.
- [50] a) H. Deng, S. L. Cobb, A. R. McEwan, R. P. McGlinchey, J. H. Naismith, D. O'Hagan, D. A. Robinson, J. B. Spencer, *Angew. Chem. Int. Ed. Engl.* **2006**, *45*, 759–762; b) S. Thompson, I. N. Fleming, D. O'Hagan, *Org. Biomol. Chem.* **2016**, *14*, 3120–3129; c) Q. Zhang, S. Dall'Angelo, I. N. Fleming, L. F. Schweiger, M. Zanda, D. O'Hagan, *Chem. Eur. J.* **2016**, *22*, 10998–11004; d) P. T. Lowe, S. Dall'Angelo, T. Mulder-Krieger, I. J. Ap, M. Zanda, D. O'Hagan, *ChemBioChem* **2017**, *18*, 2156–2164.
- [51] T. Liu, C. Liu, X. Xu, F. Liu, X. Guo, N. Li, X. Wang, J. Yang, X. Yang, H. Zhu, Z. Yang, *J. Nucl. Med.* **2019**.
- [52] a) C. A. D'Souza, W. J. McBride, R. M. Sharkey, L. J. Todaro, D. M. Goldenberg, *Bioconjugate Chem.* **2011**, *22*, 1793–1803; b) S. Boschi, J. T. Lee, S. Beykan, R. Slavik, L. Wei, C. Spick, U. Eberlein, A. K. Buck, F. Lodi, G. Cicoria, J. Czernin, M. Lassmann, S. Fanti, K. Herrmann, *Eur. J. Nucl. Med. Mol. Imaging* **2016**, *43*, 2122–2130.
- [53] N. Harada, H. Kimura, S. Onoe, H. Watanabe, D. Matsuoka, K. Arimitsu, M. Ono, H. Saji, *J. Nucl. Med.* **2016**, *57*, 1978–1984.
- [54] a) G. Vaidyanathan, M. R. Zalutsky, *Nat. Protoc.* **2006**, *1*, 1655–1661; b) J. Marik, J. L. Sutcliffe, *Appl. Radiat. Isot.* **2007**, *65*, 199–203; c) G. Tang, W. Zeng, M. Yu, G. Kabalka, *J. Label. Compd. Radiopharm.* **2008**, *51*, 68–71; d) D. Thonon, D. Goblet, E. Goukens, G. Kaisin, J. Paris, J. Aerts, S. Lignon, X. Franci, R. Hustinx, A. Luxen, *Mol. Imaging Biol.* **2011**, *13*, 1088–1095; e) P. Johnstrom, J. C. Clark, J. D. Pickard, A. P. Davenport, *Nucl. Med. Biol.* **2008**, *35*, 725–731.
- [55] a) N. Harada, H. Kimura, M. Ono, H. Saji, *J. Med. Chem.* **2013**, *56*, 7890–7901; b) K. Wakisaka, Y. Arano, T. Uezono, H. Akizawa, M. Ono, K. Kawai, Y. Ohomomo, M. Nakayama, H. Saji, *J. Med. Chem.* **1997**, *40*, 2643–2652.
- [56] V. Bouvet, M. Wuest, H. S. Jans, N. Janzen, A. R. Genady, J. F. Valliant, F. Benard, F. Wuest, *EJNMMI Res.* **2016**, *6*, 40.
- [57] G. Lu, K. P. Maresca, S. M. Hillier, C. N. Zimmerman, W. C. Eckelman, J. L. Joyal, J. W. Babich, *Bioorg. Med. Chem. Lett.* **2013**, *23*, 1557–1563.
- [58] a) S. A. Kularatne, Z. Zhou, J. Yang, C. B. Post, P. S. Low, *Mol. Pharm.* **2009**, *6*, 790–800; b) S. M. Hillier, K. P. Maresca, G. Lu, R. D. Merkin, J. C. Marquis, C. N. Zimmerman, W. C. Eckelman, J. L. Joyal, J. W. Babich, *J. Nucl. Med.* **2013**, *54*, 1369–1376.

- [59] S. Robu, A. Schmidt, M. Eiber, M. Schottelius, T. Gunther, B. Hooshyar Yousefi, M. Schwaiger, H. J. Wester, *EJNMMI Res.* **2018**, *8*, 30.
- [60] S. P. Rowe, M. A. Gorin, M. E. Allaf, K. J. Pienta, P. T. Tran, M. G. Pomper, A. E. Ross, S. Y. Cho, *Prostate Cancer Prostatic Dis.* **2016**, *19*, 223–230.
- [61] C. Barinka, K. Hlouchova, M. Rovenska, P. Majer, M. Dauter, N. Hin, Y. S. Ko, T. Tsukamoto, B. S. Slusher, J. Konvalinka, J. Lubkowski, *J. Mol. Biol.* **2008**, *376*, 1438–1450.
- [62] M. Benesova, U. Bauder-Wust, M. Schafer, K. D. Klika, W. Mier, U. Haberkorn, K. Kopka, M. Eder, *J. Med. Chem.* **2016**, *59*, 1761–1775.
- [63] T. Wustemann, U. Bauder-Wust, M. Schafer, M. Eder, M. Benesova, K. Leotta, C. Kratochwil, U. Haberkorn, K. Kopka, W. Mier, *Theranostics* **2016**, *6*, 1085–1095.
- [64] a) M. Studer, C. F. Meares, *Bioconjugate Chem.* **1992**, *3*, 337–341; b) F. Roesch, P. J. Riss, *Curr. Top. Med. Chem.* **2010**, *10*, 1633–1668.
- [65] S. Ray Banerjee, Z. Chen, M. Pullambhatla, A. Lisok, J. Chen, R. C. Mease, M. G. Pomper, *Bioconjugate Chem.* **2016**, *27*, 1447–1455.
- [66] S. H. Moon, M. K. Hong, Y. J. Kim, Y. S. Lee, D. S. Lee, J. K. Chung, J. M. Jeong, *Bioorg. Med. Chem.* **2018**, *26*, 2501–2507.
- [67] W. J. Oyen, J. S. de Bono, *J. Nucl. Med.* **2016**, *57*, 1838–1839.
- [68] a) M. R. McDevitt, D. Ma, J. Simon, R. K. Frank, D. A. Scheinberg, *Appl. Radiat. Isot.* **2002**, *57*, 841–847; b) J. Fitzsimmons, R. Atcher, *J. Label. Compd. Radiopharm.* **2007**, *50*, 147–153.
- [69] J. M. Kelly, A. Amor-Coarasa, A. Nikolopoulou, D. Kim, C. Williams, Jr., S. Vallabhajosula, J. W. Babich, *Nucl. Med. Biol.* **2017**, *55*, 38–46.
- [70] J. Notni, J. Simecek, P. Hermann, H. J. Wester, *Chem. Eur. J.* **2011**, *17*, 14718–14722.
- [71] D. Reich, A. Wurzer, M. Wirtz, V. Stiegler, P. Spatz, J. Pollmann, H. J. Wester, J. Notni, *Chem. Commun.* **2017**, *53*, 2586–2589.
- [72] A. Wurzer, C. Seidl, A. Morgenstern, F. Bruchertseifer, M. Schwaiger, H. J. Wester, J. Notni, *Chem. Eur. J.* **2018**, *24*, 547–550.
- [73] J. Notni, J. Simecek, H. J. Wester, *ChemMedChem* **2014**, *9*, 1107–1115.
- [74] J. Simecek, P. Hermann, J. Havlickova, E. Herdtweck, T. G. Kapp, N. Engelbogen, H. Kessler, H. J. Wester, J. Notni, *Chem. Eur. J.* **2013**, *19*, 7748–7757.
- [75] a) J. Notni, P. Hermann, J. Havlickova, J. Kotek, V. Kubicek, J. Plutnar, N. Loktionova, P. J. Riss, F. Rosch, I. Lukes, *Chem. Eur. J.* **2010**, *16*, 7174–7185; b) V. Smetana, G. J. Miller, J. D. Corbett, *Inorg. Chem.* **2012**, *51*, 7711–7721.
- [76] A. Wurzer, J. Pollmann, A. Schmidt, D. Reich, H. J. Wester, J. Notni, *Mol. Pharmaceutics* **2018**, *15*, 4296–4302.
- [77] H. L. Handl, J. Vagner, H. Han, E. Mash, V. J. Hruby, R. J. Gillies, *Expert Opin. Ther. Targets* **2004**, *8*, 565–586.
- [78] G. Vauquelin, S. J. Charlton, *Br. J. Pharmacol.* **2013**, *168*, 1771–1785.
- [79] H. M. Shallal, I. Minn, S. R. Banerjee, A. Lisok, R. C. Mease, M. G. Pomper, *Bioconjugate Chem.* **2014**, *25*, 393–405.
- [80] S. R. Banerjee, C. A. Foss, M. Castanares, R. C. Mease, Y. Byun, J. J. Fox, J. Hilton, S. E. Lupold, A. P. Kozikowski, M. G. Pomper, *J. Med. Chem.* **2008**, *51*, 4504–4517.
- [81] J. P. Xiong, T. Stehle, R. Zhang, A. Joachimiak, M. Frech, S. L. Goodman, M. A. Arnaout, *Science* **2002**, *296*, 151–155.
- [82] M. Subedi, I. Minn, J. Chen, Y. Kim, K. Ok, Y. W. Jung, M. G. Pomper, Y. Byun, *Eur. J. Med. Chem.* **2016**, *118*, 208–218.
- [83] Z. Wang, R. Tian, G. Niu, Y. Ma, L. Lang, L. P. Szajek, D. O. Kiesewetter, O. Jacobson, X. Chen, *Bioconjugate Chem.* **2018**, *29*, 3213–3221.
- [84] a) H. Chen, O. Jacobson, G. Niu, I. D. Weiss, D. O. Kiesewetter, Y. Liu, Y. Ma, H. Wu, X. Chen, *J. Nucl. Med.* **2017**, *58*, 590–597; b) R. Tian, O. Jacobson, G. Niu, D. O. Kiesewetter, Z. Wang, G. Zhu, Y. Ma, G. Liu, X. Chen, *Theranostics* **2018**, *8*, 735–745.
- [85] R. Y. Tsien, *Nat. Rev. Mol. Cell Biol.* **2003**, *Suppl*, SS16–SS21.
- [86] a) S. Lutje, M. Rijpkema, G. M. Franssen, G. Fracasso, W. Helfrich, A. Eek, W. J. Oyen, M. Colombatti, O. C. Boerman, *J. Nucl. Med.* **2014**, *55*, 995–1001; b) A. C. Baranski, M. Schafer, U. Bauder-Wust, M. Roscher, J. Schmidt, E. Stenau, T. Simpfendorfer, D. Teber, L. Maier-Hein, B. Hadaschik, U. Haberkorn, M. Eder, K. Kopka, *J. Nucl. Med.* **2018**, *59*, 639–645.
- [87] H. Kommidi, H. Guo, F. Nurili, Y. Vedvyas, M. M. Jin, T. D. McClure, B. Ehdai, H. B. Sayman, O. Akin, O. Aras, R. Ting, *J. Med. Chem.* **2018**, *61*, 4256–4262.
- [88] Z. Liu, M. Pourghasian, M. A. Radtke, J. Lau, J. Pan, G. M. Dias, D. Yapp, K. S. Lin, F. Benard, D. M. Perrin, *Angew. Chem. Int. Ed. Engl.* **2014**, *53*, 11876–11880.
- [89] A. Kumar, T. Mastren, B. Wang, J. T. Hsieh, G. Hao, X. Sun, *Bioconjugate Chem.* **2016**, *27*, 1681–1689.
- [90] a) R. V. Chari, M. L. Miller, W. C. Widdison, *Angew. Chem. Int. Ed. Engl.* **2014**, *53*, 3796–3827; b) N. Krall, F. Pretto, W. Decurtins, G. J. Bernardes, C. T. Supuran, D. Neri, *Angew. Chem. Int. Ed. Engl.* **2014**, *53*, 4231–4235.
- [91] a) R. P. Murelli, A. X. Zhang, J. Michel, W. L. Jorgensen, D. A. Spiegel, *J. Am. Chem. Soc.* **2009**, *131*, 17090–17092; b) A. Dubrovska, C. Kim, J. Elliott, W. Shen, T. H. Kuo, D. I. Koo, C. Li, T. Tuntland, J. Chang, T. Groessl, X. Wu, V. Gorney, T. Ramirez-Montagut, D. A. Spiegel, C. Y. Cho, P. G. Schultz, *ACS Chem. Biol.* **2011**, *6*, 1223–1231.
- [92] A. R. Genady, N. Janzen, L. Banevicius, M. El-Gamal, M. E. El-Zaria, J. F. Valliant, *J. Med. Chem.* **2016**, *59*, 2660–2673.
- [93] X. Yang, R. C. Mease, M. Pullambhatla, A. Lisok, Y. Chen, C. A. Foss, Y. Wang, H. Shallal, H. Edelman, A. T. Hoye, G. Attardo, S. Nimmagadda, M. G. Pomper, *J. Med. Chem.* **2016**, *59*, 206–218.
- [94] C. Barinka, Z. Novakova, N. Hin, D. Bim, D. V. Ferraris, B. Duvall, G. Kabarriti, R. Tsukamoto, M. Budesinsky, L. Motlova, C. Rojas, B. S. Slusher, T. A. Rokob, L. Rulisek, T. Tsukamoto, *Bioorg. Med. Chem.* **2019**, *27*, 255–264.

Manuscript received: June 5, 2019
Revised manuscript received: July 16, 2019
Accepted manuscript online: July 26, 2019
Version of record online: August 27, 2019